



Multimodal Heartbeat and Compression Optical Coherence Elastography for Mapping Corneal Biomechanics

Achuth Nair¹, Manmohan Singh¹, Salavat R. Aglyamov² and Kirill V. Larin^{1,3*}

¹ Biomedical Engineering, University of Houston, Houston TX, United States, ² Mechanical Engineering, University of Houston, Houston TX, United States, ³ Molecular Physiology and Biophysics, Baylor College of Medicine, Houston, TX, United States

OPEN ACCESS

Edited by:

Bernardo Yanez-Soto,
Universidad Autónoma de San Luis
Potosí, Mexico

Reviewed by:

Jun Liu,
The Ohio State University,
United States
Cuiru Sun,
Tianjin University, China

*Correspondence:

Kirill V. Larin
klarin@uh.edu

Specialty section:

This article was submitted to
Ophthalmology,
a section of the journal
Frontiers in Medicine

Received: 11 December 2021

Accepted: 28 February 2022

Published: 05 April 2022

Citation:

Nair A, Singh M, Aglyamov SR
and Larin KV (2022) Multimodal
Heartbeat and Compression Optical
Coherence Elastography for Mapping
Corneal Biomechanics.
Front. Med. 9:833597.
doi: 10.3389/fmed.2022.833597

The biomechanical properties of the cornea have a profound influence on the health, structural integrity, and function of the eye. Understanding these properties may be critical for diagnosis and identifying disease pathogenesis. This work demonstrates how two different elastography techniques can be combined for a multimodal approach to measuring corneal biomechanical properties. Heartbeat optical coherence elastography (Hb-OCE) and compression OCE were performed simultaneously to measure the stiffness of the cornea in an *in vivo* rabbit model. Measurements were further performed after collagen crosslinking to demonstrate how the combined technique can be used to measure changes in corneal stiffness and map mechanical contrast. The results of this work further suggest that measurements from Hb-OCE and compression OCE are comparable, meaning that Hb-OCE and compression OCE may be used interchangeably despite distinct differences in both techniques.

Keywords: optical coherence elastography (OCE), optical coherence tomography (OCT), biomechanics, cornea, elasticity

INTRODUCTION

It is well-established that assessing the mechanical properties of the cornea can help diagnose ocular pathologies or evaluate therapeutic intervention (1, 2). Clinical tools for this assessment include the Corvis ST and the Ocular Response Analyzer (ORA) (3). These tools analyze the corneal response to a large amplitude air puff to assess tissue mechanical properties. However, the large bulk motion and the non-physiological deformation of the cornea results in misleading measurements of mechanical properties (4). As such, alternative tools that can perform a more robust assessment of corneal biomechanical properties are needed.

Elastography has been demonstrably effective for *in vivo* assessment of corneal mechanical properties. Ultrasound elastography has been previously performed in humans using ultrasound surface wave elastography (USWE) and ocular pulse elastography (OPE) (5, 6). However, ultrasonic shear wave techniques typically suffer from poor contrast and a low resolution that can limit their effectiveness for imaging the small, thin ocular tissues. OPE improves on shear wave methods particularly in terms of displacement resolution and sensitivity due to the use of radiofrequency data and interpolation. Furthermore, OPE has been used to successfully distinguish stiffness

between untreated and corneal collagen crosslinked human corneas, and represents a significant step forward in approaching the displacement sensitivity of optical imaging techniques (7, 8). Alternatively, Brillouin microscopy has been used to measure the mechanical properties of the cornea *in vivo* (9). However, this technique has long imaging times, and the relationship between the Brillouin modulus and Young's modulus is still under investigation.

Optical coherence elastography presents another alternative for evaluating biomechanical properties of the cornea *in vivo*. Various techniques, including wave-based OCE, have been performed successfully in humans (10, 11). Compression OCE has been demonstrated in humans as well and has been effective in quantifying mechanical contrast between corneas in healthy subjects and patients with keratoconus (12). In addition to these human studies, both dynamic and quasi-static OCE has been performed in animal studies *in vivo* (13–15). Additionally, passive OCE, a method that involves the use of physiological processes to induce displacement, has also been utilized to study the mechanical properties of the cornea *in vivo* (16, 17). However, OCE has technical challenges as well. Limitations in OCT imaging depth and signal sensitivity rolloff can restrict measurements to the central region of the cornea. Traditional OCT systems also have comparably slower acquisitions speeds compared to other elastography methods, such as ultrasound, which makes real time assessment of elasticity challenging. However, recent advances in OCE using high speed OCT systems seek to overcome some of these obstacles (18, 19).

In this work, we demonstrate a multimodal OCE technique to map the mechanical properties of the cornea that combines a passive technique, heartbeat OCE (Hb-OCE) (17, 20), with an active technique, compression OCE (15, 21). Previously, multimodal optical elastography has only been performed using a combined Brillouin microscopy and OCE system to evaluate the mechanical properties of the crystalline lens (22). However, both techniques were performed separately, and the results were combined for analysis. Here, we demonstrate synchronous multimodal optical elastography for the first time, where both Hb-OCE and compression OCE were used to measure corneal mechanical properties simultaneously. Both methods are quasi-static semi-quantitative (comparable within a region of interest acquired in one measurement) techniques subject to a slow-rate displacement. However, with compression OCE, that displacement comes from a mechanical actuator. In Hb-OCE, the displacement comes in the form of the ocular pulse (23). Here, we demonstrate how a multimodal technique might be used *in vivo* and investigate how these two distinct OCE techniques compare to one another.

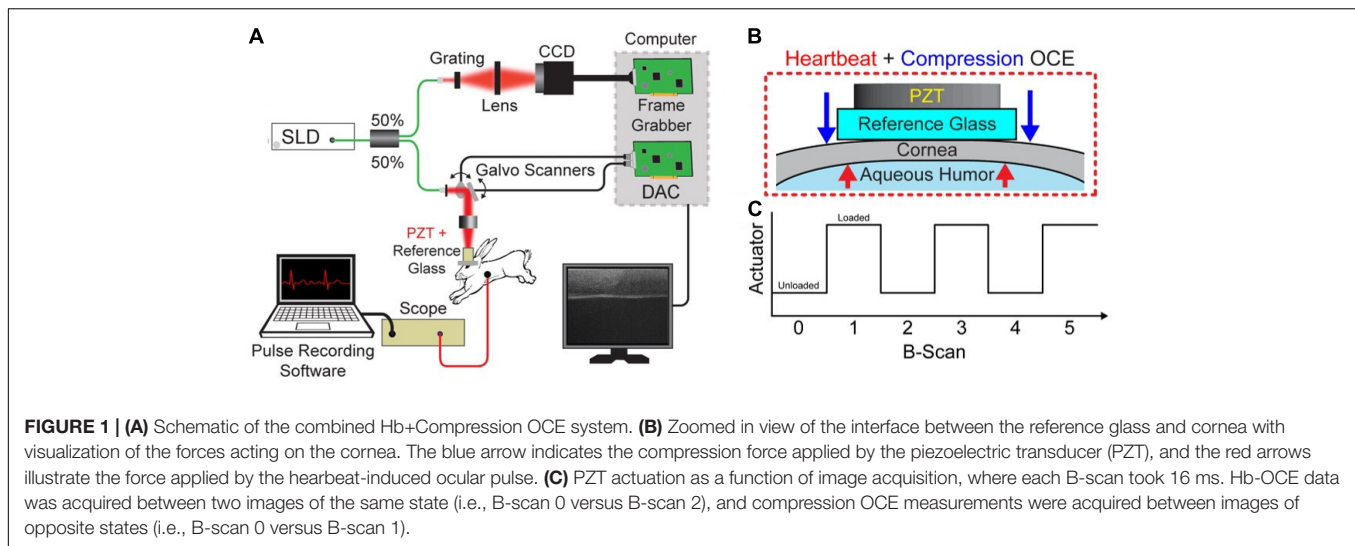
MATERIALS AND METHODS

Measurements were performed in adult male Dutch-Belted rabbits ($n = 3$). Animals were anesthetized with an initial intramuscular dose of 40 mg/kg ketamine and 5 mg/kg xylazine by a veterinarian. IOP measurements were acquired with a handheld rebound tonometer (Tonovet, Icare Finland Oy,

Vantaa, Finland). Animals were placed in a lateral recumbent position in a custom-made rest with a heating pad to ensure that the animals remained at a comfortable temperature throughout the experiments. Vital signs were monitored by a veterinarian, and a maintenance dose of 20 mg/kg ketamine was injected as needed intramuscularly. A three-axis stage was used for orientating the animal under the OCT sample arm. During the procedure, the rabbits were unable to blink, so a solution of 1X phosphate-buffered saline (PBS) was applied topically at regular intervals to maintain corneal hydration. All animal procedures were approved by the University of Houston Institutional Animal Care and Use Committee.

The acquisition was performed with a spectral-domain OCT system with 840-nm central wavelength, 49-nm bandwidth, 6- μm axial resolution, and 8- μm lateral resolution operating at a 62.5-kHz line rate. B-M-mode scans of 1000 A-lines were acquired over a ~ 2.5 mm region across the apex of the cornea. A hollow cylindrical piezoelectric actuator (HPSt 150/14–10/12 Piezomechanik GmbH, Munich, Germany) mounted to a reference glass was aligned with the OCT sample arm in the common path configuration. Common-path imaging combined with phase-sensitive measurements enabled sub-nanometer displacement sensitivity (21, 24, 25). A small drop of oil was applied to the cornea for lubrication, and the OCT sample arm was lowered onto the cornea until the tissue was appanated within the 2.5 mm field of view. The actuator was synchronized with the OCT frame trigger such that one image was acquired when the tissue was uncompressed, and the next image was acquired when the tissue was compressed (26). As such, compression occurred at the B-scan rate of ~ 62 Hz. This low frequency excitation ensures that there was a minimal effect of viscosity on measurements. Cardiac activity was monitored through the imaging procedure for Hb-OCE measurements using a pressure transducer (PowerLab, ADInstruments, Dunedin, New Zealand) that was placed on the rabbit chest. The heartbeat data was later temporally coregistered with the OCE data by synchronizing the pressure measurements with the time stamps of the OCT images. **Figure 1** below shows the schematic of the combined Hb-Compression OCE system, including forces acting upon the cornea and the image acquisition protocol in terms of actuator loading. Compression OCE analysis was performed by comparing images between the compressed and uncompressed states (i.e., B-scan 0 versus B-scan 1 in **Figure 1A**). On the other hand, Hb-OCE acquisition was performed by comparing OCT images within the same state (i.e., B-scan 0 versus B-scan 2). That leads to an effective B-scan rate of ~ 62 Hz for the compression OCE measurements, and ~ 31 Hz for Hb-OCE. Since the typical rabbit heart rate is within the range of 3–4 Hz, Hb-OCE measurements were acquired at approximately 10x the heart rate. Images were acquired over 12 s so that multiple cardiac cycles could be acquired, and the corneal strain as a function of time could be detected.

The OCE data were analyzed using a technique described in our previous works (15, 17). Briefly, motion between samples was detected by computing the phase difference between successive frames for analysis using a complex conjugate method (27). Next, a vector averaging method using an isometric 15 μm kernel was



used to reduce noise in the phase difference image (28). Phase data, φ , was translated into displacement d using the following relationship,

$$d = \frac{\varphi\lambda_0}{4\pi n}, \quad (1)$$

where, λ_0 was the central wavelength of the OCT system, and n was the refractive index, considered to be 1.376 in the cornea (29). The OCT displacement stability was measured to be less than <0.5 nm at a signal to noise ratio of 65 dB (20). The strain was calculated using a least-squares regression algorithm along every A-line in the displacement image within an isometric window with a size of $75 \mu\text{m}$ (30). Regions at the periphery of the field of view with poor contact with the reference glass were not included in the analysis. Hb-OCE measurements were temporally filtered at the heart rate measured by the pressure transducer, then mapped and quantified based on the peak strain averaged over 12 cardiac cycles. On the other hand, compression OCE images were calculated based on mean strain within the same period. Thus, the analysis was performed on data acquired at the same time.

To compare the capabilities of both techniques for assessing changes in corneal stiffness and mapping mechanical heterogeneity, UV-A/riboflavin corneal collagen crosslinking (CXL) was performed on the corneas using the standard Dresden protocol following measurement of the untreated cornea (31). Therefore, of the three animals used for measurements, $n = 6$ eyes were used for untreated measurements, and $n = 2$ eyes, one eye from each of two animals, were utilized for crosslinked measurements. Data from one virgin cornea was removed due to poor contact with the reference glass. Due to the low sample size of CXL corneas, inter-sample statistical testing was not performed. Changes in stiffness due to CXL were assessed using intra-sample statistical testing, as each image pixel indicates a unique measurement. Briefly, the corneal epithelium was removed, and a solution of 0.1% riboflavin in 20% dextran was topically applied to the surface of the cornea in 5-minute

intervals for 60 min. After 30 min of riboflavin instillation, the surface of the cornea was irradiated with UV light (365 nm , 3 mW/cm^2). Partial CXL was also performed in one cornea by limiting the UV irradiation area to a localized region of the cornea. The raw partial CXL data was also utilized in a previous publication (15).

RESULTS

Figure 2A shows the OCT intensity B-scan of a representative virgin cornea. The compressive strain measured by Hb-OCE and compression OCE are shown in **Figures 2B,C**, respectively. Both corneas show a slight degree of spatial heterogeneity, as expected. **Figure 2D** shows a direct comparison between Hb-OCE and compression OCE measurements ($n = 5$ virgin and $n = 2$ CXL corneas). The inter-sample mean compressive strain measured by Hb-OCE was $0.16 \pm 0.9 \text{ m}\epsilon$, and $0.16 \pm 0.6 \text{ m}\epsilon$ measured by compression OCE. The measurements from Hb-OCE and compression OCE were statistically insignificant by a paired t -test ($p = 0.96$).

Figure 3A shows the OCT intensity B-scan of the cornea from **Figure 2A** that has undergone CXL. Note the increase in scattering after CXL as compared to **Figure 2A** as well as the decrease in the overall thickness of the tissue, consistent with our previous results with CXL (32). **Figures 3B,C** illustrate the compressive strain in the cornea measured by Hb-OCE and compression OCE, again showing an overall spatial homogeneity in the cornea. Strain is noticeably lower with both measurements techniques when compared to the cornea before the CXL treatment in **Figure 2**. Because there were only two samples in the crosslinking group, inter-sample statistical testing would not provide meaningful information. As such, **Figure 3D** shows the corneal strain measured by Hb-OCE and compression OCE of the same cornea before and after CXL. The mean compressive strain measured by Hb-OCE in the virgin cornea was $0.17 \pm 0.06 \text{ m}\epsilon$ and $0.07 \pm 0.02 \text{ m}\epsilon$ in the CXL cornea. The mean compressive strain measured by compression OCE was $0.22 \pm 0.08 \text{ m}\epsilon$ in the

virgin cornea and 0.10 ± 0.06 mε in the CXL cornea. A paired *t*-test showed a statistically insignificant difference between Hb-OCE measurements and compression OCE measurements in the virgin corneas ($p = 0.79$), and a statistically insignificant difference between both OCE techniques in the CXL cornea ($p = 0.87$). However, both Hb-OCE and compression-OCE showed a statistically significant difference between untreated and crosslinked tissues by a paired *t*-test ($p < 0.01$ and $p = 0.038$, respectively). Both methods also demonstrated a greater than 60% increase in the stiffness of both corneas after crosslinking was performed, which is within expectations (15).

Figure 4 illustrates the results of both Hb-OCE and compression OCE in a partially crosslinked rabbit cornea. **Figure 4A** shows the OCT intensity B-scan, where the dotted regions are the calculation windows of the (red) CXL and (blue) virgin regions. **Figures 4B,C** illustrate the compressive strain map obtained by Hb-OCE and compression OCE, respectively. Both maps show a distinct difference in corneal strain between the CXL and virgin regions. **Figure 4D** plots the mean compressive strain measured by Hb-OCE and compression OCE in the virgin and CXL regions. Hb-OCE measured a mean compressive strain of 0.32 ± 0.07 mε in the virgin region and a mean compressive strain of 0.18 ± 0.05 mε in the CXL region. Compression OCE measured a mean compressive strain of 0.41 ± 0.13 mε in the virgin region and 0.20 ± 0.07 mε in the CXL region. A paired *t*-test showed a statistically insignificant difference between Hb-OCE and compression OCE measurements in both the virgin ($p = 0.58$) and CXL ($p = 0.08$) regions. However, between the untreated and CXL regions, both Hb-OCE ($p < 0.01$) and compression OCE ($p = 0.007$) showed a statistically significant difference. Hb-OCE showed a 43% increase in stiffness after CXL, and compression OCE showed a 56% increase in stiffness after CXL.

DISCUSSION

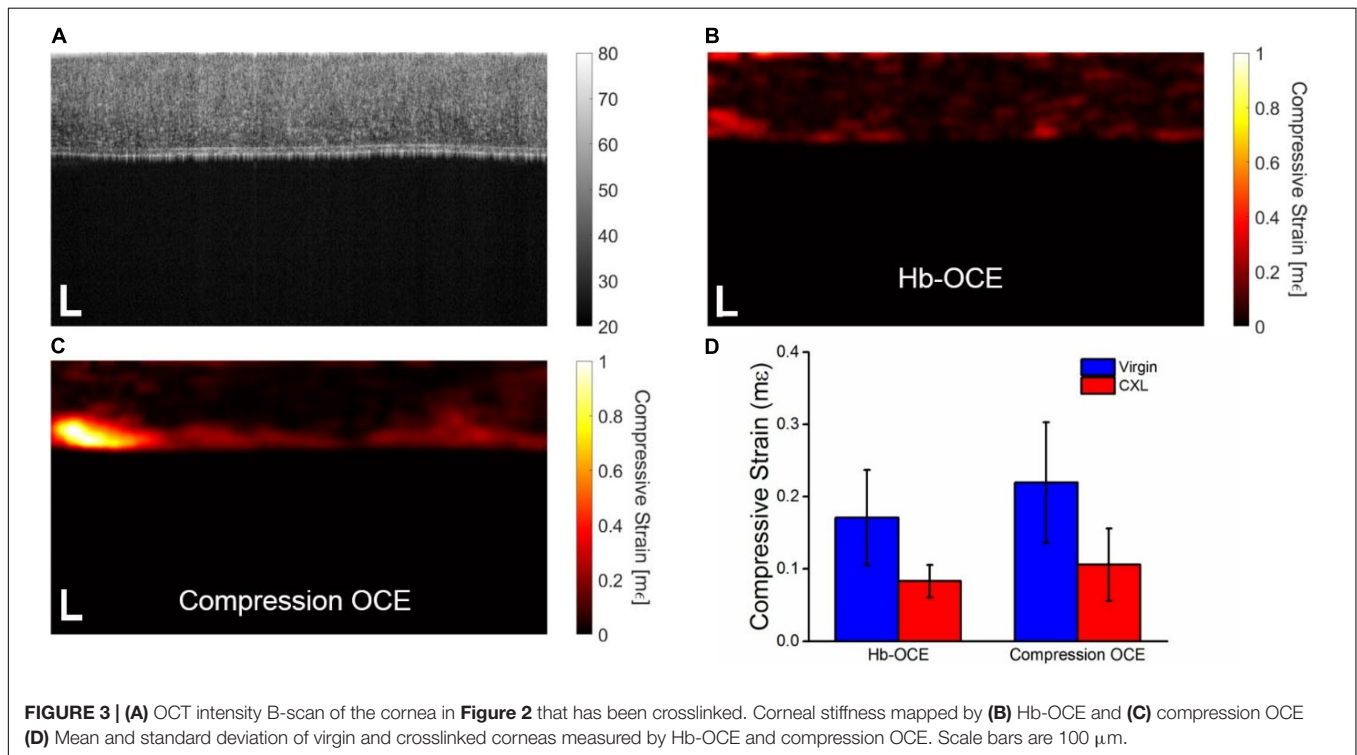
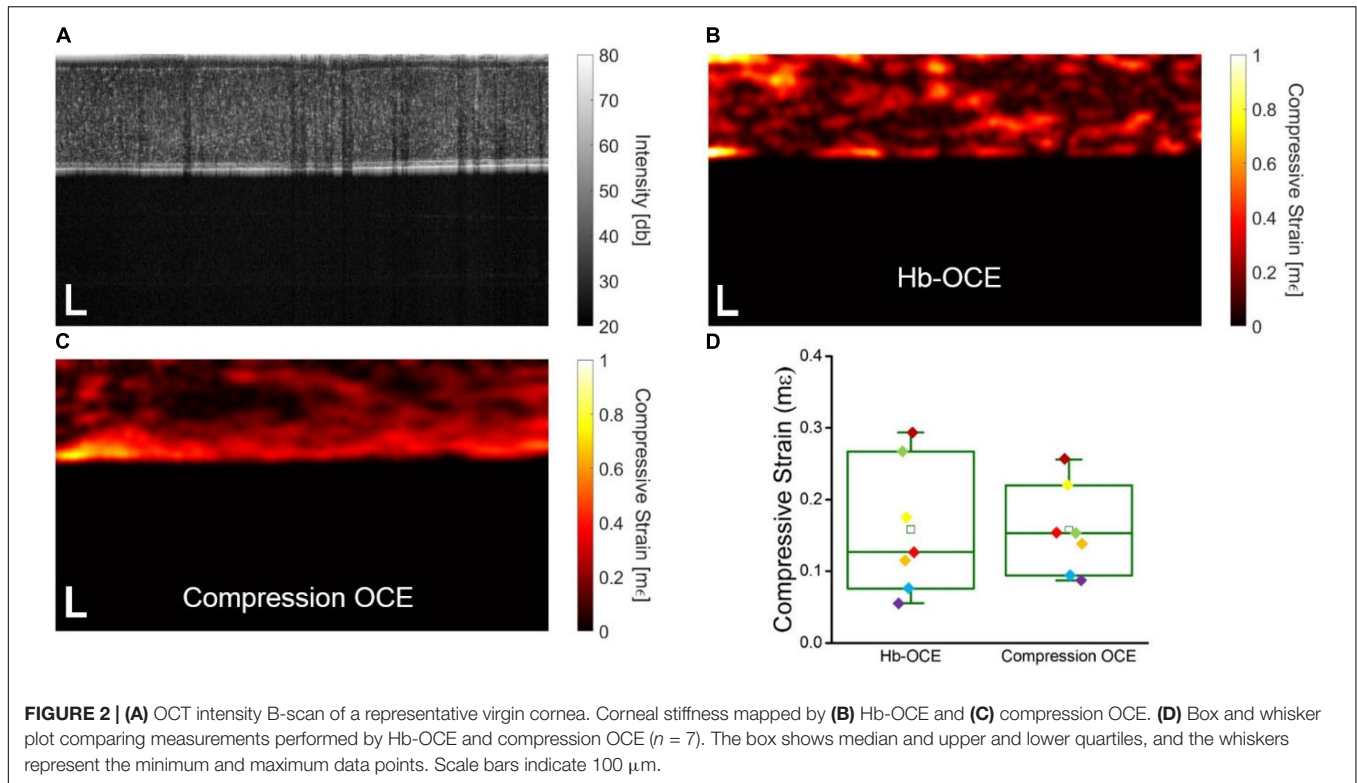
In this work, we performed a pilot study to demonstrate the first use of multimodal OCE using a simultaneous acquisition to our knowledge. Hb-OCE and compression OCE have been previously used to measure the biomechanical properties of the cornea *in vivo*, and though both methods can be useful to provide semi-quantitative information regarding corneal biomechanical properties, the techniques have not been compared to one another directly despite their similarities. Hb-OCE and compression OCE are distinguished by two primary factors. First, displacement in Hb-OCE is passively induced by the ocular pulse, whereas in compression OCE, displacement is actively induced using a mechanical actuator. As a result, in this work, mechanical actuation in compression OCE occurs ~14x faster than heart rate, which is beneficial for patient comfort. Second, in Hb-OCE, the displacement occurs from within the aqueous humor below the cornea, and in compression OCE, the displacement occurs from above the tissue. Finally, the stress and subsequent displacement induced by the mechanical actuator is far more easily controlled and repeatable due to its electro-mechanical nature as compared to the ocular pulse.

Despite these differences, based on the results of **Figure 2**, mean strains from Hb-OCE and compression OCE are statistically insignificant, suggesting that both measurement techniques may effectively provide equivalent information despite their differences. Presumably, this was because the ocular pulse stress and the PZT stress were very similar, resulting in similar strains. This finding suggests that Hb-OCE may be a suitable passive replacement for compression OCE for mapping corneal strains and vice versa. The current study has a limited sample size, with multiple measurements being performed on three animals. While the data here does suggest certain trends, it is important to note that future studies involving a larger sample size are required to obtain more conclusive results.

The results described in **Figure 3** further support that Hb-OCE and compression OCE may provide comparable measurements. Hb-OCE and compression OCE were used to compare the change in corneal stiffness after CXL. While both techniques showed a significant difference between virgin and crosslinked corneas, there was not a significant difference between measurements performed by either technique. We can see this occurrence in **Figure 4** as well in a partially crosslinked cornea. While there is a statistically significant difference between both regions measured by both techniques, the difference between techniques for a particular region is still insignificant. Furthermore, while compression OCE has been used to map mechanical contrast in corneas *in vivo* (15), **Figure 4** shows the first use of Hb-OCE for the task.

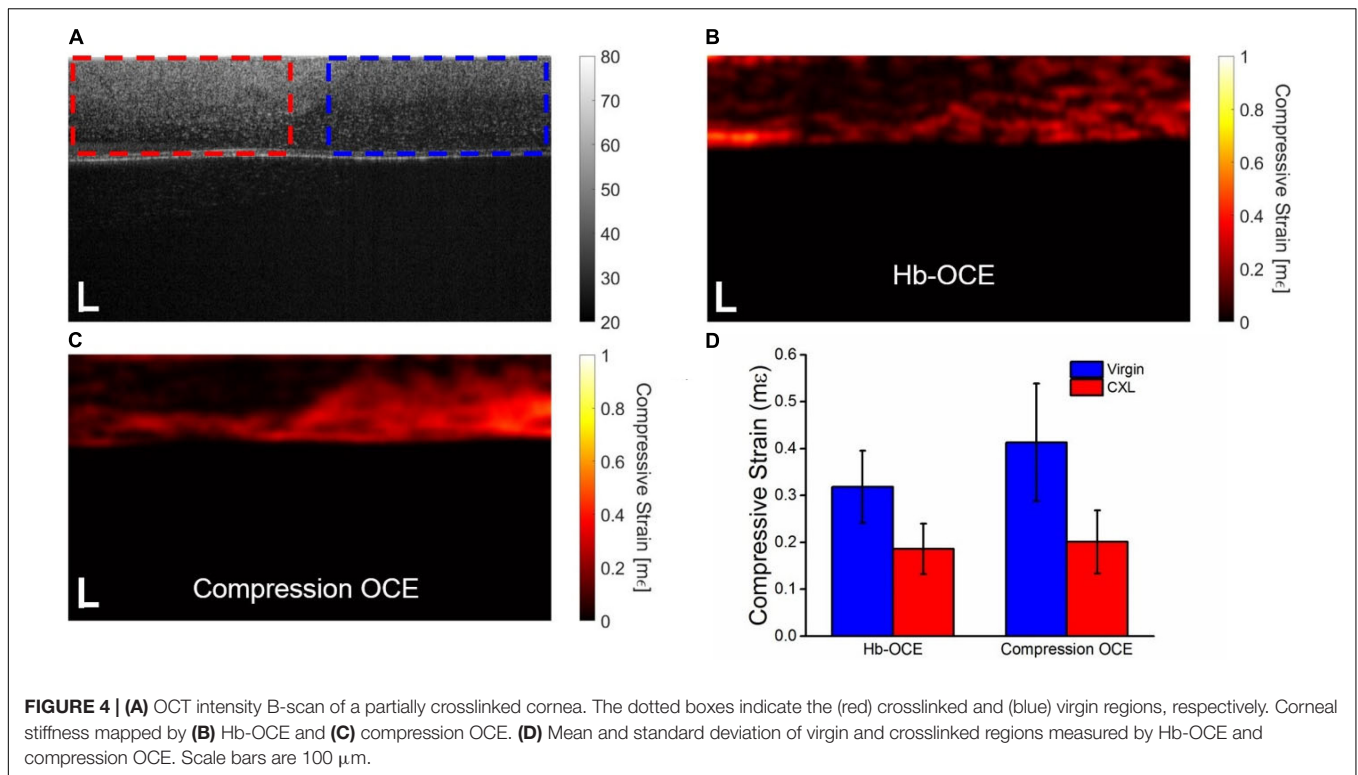
However, our results also suggest certain limitations. The results of our work show significant variance in compressive strain measured by compression OCE, which is highlighted in **Figures 3, 4**. This variance is likely due to axial variation in stiffness between the anterior and posterior segments of the cornea (15). Furthermore, variances may be due to noise introduced by additive numerical errors from each step of the calculation, which will be addressed in future improvements to the strain calculation algorithm. It should be noted that the increased corneal strain around the endothelium shown in the compression OCE strain maps is likely due to edge artifacts related to the strain calculation and was not used for statistical analysis. Compression OCE has been previously used to demonstrate differences between these two regions (15); however, it is less clear from these results if Hb-OCE can distinguish these regions. On the other hand, Hb-OCE shows significantly less variance from the mean compressive strain. This is largely in part due to the slightly reduced displacement of Hb-OCE (0.05 ± 0.03 μm) compared to compression OCE (0.07 ± 0.04 μm), which may not reach all the way through the cornea. In fact, while mechanical resolution and sensitivity have been investigated in compression OCE (33, 34), neither has been evaluated for *in vivo* quasi-static OCE. Further investigation will be needed to clarify.

Our study is also subject to measurement limitations as well. Direct appplanation of the cornea, as shown here, may not be comfortable for a patient. However, Goldmann appplanation tonometry (GAT) is typically performed with a topical anesthetic, although GAT was well tolerated even without anesthetic (35). Furthermore, there is precedence for appplanating the cornea for



OCE (12, 36). Additionally, applanation is known to alter the IOP of the eye globe, and due to the relationship between IOP, ocular pulse amplitude, and the Hb-OCE measurements, this change in IOP must be accounted for. In our measurements of

Hb-OCE, we allow the eye globe enough time to stabilize so that transient changes in IOP due to the applanation process have limited effects on the Hb-OCE measurements. Finally, this study has been limited to the 2D mapping of axial strains, however



various algorithms have been developed to assess lateral and axial strains using compression OCE (37, 38). Future work will investigate how these algorithms can be implemented into Hb-OCE measurements. Beyond 2D mapping of corneal stiffness, 3D mapping would be even more valuable. Mapping corneal strain in 3D using compression OCE may require considerable acquisition times with the current setup, and 3D Hb-OCE is still under investigation. However, ultra-fast OCE techniques may be able to limit or even eliminate the increase in imaging time going from 2D to 3D measurements (18, 19). Furthermore, while this study focuses on the measurement of axial strain, further developing compression OCE and Hb-OCE with 3D applications is an avenue of our future work.

Here, we performed semi-quantitative mapping of corneal biomechanical properties using a multimodal Hb-OCE and compression OCE technique. However, because strain is a semi-quantitative metric, comparisons between samples based on strain are innately limited. To translate these measurements to truly quantitative results, we need to quantify the stress acting upon the cornea due to either compression or the ocular pulse in addition to the strain. One way to perform this assessment is by quantifying the IOP *in vivo*, which may be performed using dynamic contour tonometry (6). Measuring the change in IOP as a response to the compression OCE measurement or recording the change in IOP due to the ocular pulse could be useful in quantifying corneal stress and translating strain into a quantitative biomechanical parameter (15). Another option is the use of a compliant stress sensor, which has been demonstrated in previous compression OCE applications (39). A stress sensor would be especially useful for mapping heterogeneity in stress

and could provide an even more accurate measurement of stiffness using Hb-OCE and compression OCE with the added benefit of increased mechanical contrast. Furthermore, it should be noted that the corneal strain measured by Hb-OCE could be heavily influenced by the ocular pulse. Further analysis that accounts for the ocular pulse, or the stress on the cornea, would allow for more accurate comparison between these two types of measurements.

CONCLUSION

This work demonstrates multimodal Hb-OCE and compression OCE for the first time *in vivo*. Both techniques were used to measure the change in corneal stiffness after CXL and showed a similar increase in stiffness. Furthermore, both Hb-OCE and compression OCE were used to map mechanical contrast in a sample that had been partially crosslinked. Most importantly, our results showed that despite distinctly different methods of action for both techniques, the strain quantified by Hb-OCE and compression OCE were largely similar, suggesting that both techniques may be used interchangeably to measure corneal stiffness *in vivo*.

DATA AVAILABILITY STATEMENT

The raw data supporting the conclusions of this article will be made available by the authors, without undue reservation.

ETHICS STATEMENT

The animal study was reviewed and approved by UH IACUC.

AUTHOR CONTRIBUTIONS

All authors developed the concept, reviewed the data, and reviewed the manuscript.

REFERENCES

1. Pinero DP, Alcon N. Corneal biomechanics: a review. *Clin Exp Optom.* (2015) 98:107–16.
2. Kotecha A. What biomechanical properties of the cornea are relevant for the clinician?. *Surv Ophthalmol.* (2007) 52:S109–14. doi: 10.1016/j.survophthal.2007.08.004
3. Kling S, Hafezi F. Corneal biomechanics—a review. *Ophthalmic Physiol Opt.* (2017) 37:240–52.
4. Ariza-Gracia MA, Zurita JF, Pinero DP, Rodriguez-Matas JF, Calvo B. Coupled biomechanical response of the cornea assessed by non-contact tonometry. A simulation study. *PLoS One.* (2015) 10:e0121486. doi: 10.1371/journal.pone.0121486
5. Sit AJ, Lin SC, Kazemi A, McLaren JW, Pruet CM, Zhang X. In vivo noninvasive measurement of young's modulus of elasticity in human eyes: a feasibility study. *J Glaucoma.* (2017) 26:967–73. doi: 10.1097/IJG.0000000000000774
6. Kwok S, Clayson K, Hazen N, Pan X, Ma Y, Hendershot AJ, et al. Heartbeat-induced corneal axial displacement and strain measured by high frequency ultrasound elastography in human volunteers. *Transl Vis Sci Technol.* (2020) 9:33. doi: 10.1167/tvst.9.13.33
7. Clayson K, Pavlatos E, Pan X, Sandwisch T, Ma Y, Liu J. Ocular pulse elastography: imaging corneal biomechanical responses to simulated ocular pulse using ultrasound. *Transl Vis Sci Technol.* (2020) 9:5. doi: 10.1167/tvst.9.1.5
8. Pavlatos E, Chen H, Clayson K, Pan X, Liu J. Imaging corneal biomechanical responses to ocular pulse using high-frequency ultrasound. *IEEE Trans Med Imaging* (2017) 37, 663–670.
9. Scarcelli G, Besner S, Pineda R, Kalout P, Yun SH. In vivo biomechanical mapping of normal and keratoconus corneas. *JAMA Ophthalmol.* (2015) 133:480–2. doi: 10.1001/jamaophthalmol.2014.5641
10. Ramier A, Eltony AM, Chen Y, Clouser F, Birkenfeld JS, Watts A, et al. In vivo measurement of shear modulus of the human cornea using optical coherence elastography. *Sci Rep.* (2020) 10:15. doi: 10.1038/s41598-020-74383-4
11. Lan G, Aglyamov SR, Larin KV, Twa MD. In vivo human corneal shear-wave optical coherence elastography. *Optom Vis Sci.* (2021) 98:58–63. doi: 10.1097/OPX.0000000000001633
12. De Stefano VS, Ford MR, Seven I, Dupps WJ Jr. Depth-dependent corneal biomechanical properties in normal and keratoconic subjects by optical coherence elastography. *Transl Vis Sci Technol.* (2020) 9:4. doi: 10.1167/tvst.9.7.4
13. Li J, Wang S, Singh M, Aglyamov S, Emelianov S, Twa MD, et al. Air-pulse OCE for assessment of age-related changes in mouse corneal in vivo. *Laser Phys Lett.* (2014) 11:065601. doi: 10.1088/1612-2011/11/6/065601
14. Zhou Y, Wang Y, Shen M, Jin Z, Chen Y, Zhou Y, et al. In vivo evaluation of corneal biomechanical properties by optical coherence elastography at different cross-linking irradiances. *J Biomed Opt.* (2019) 24:105001. doi: 10.1117/1.JBO.24.10.105001
15. Singh M, Nair A, Aglyamov SR, Larin KV. Compressional optical coherence elastography of the cornea. *Photonics.* (2021) 8:111. doi: 10.1002/jbio.201800250

FUNDING

This research was funded by the National Institutes of Health, grant numbers R01EY022362, R01EY030063, and P30EY007551.

ACKNOWLEDGMENTS

We would like to thank Curtis Klages, Courtney Sands, Rena McMahan, and Sandra Cole for their assistance and guidance with animal care and welfare.

16. Nguyen TM, Zorgani A, Lescanne M, Boccarda C, Fink M, Catheline S. Diffuse shear wave imaging: toward passive elastography using low-frame rate spectral-domain optical coherence tomography. *J Biomed Opt.* (2016) 21:126013. doi: 10.1117/1.JBO.21.12.126013
17. Nair A, Singh M, Aglyamov S, Larin KV. Heartbeat optical coherence elastography: corneal biomechanics in vivo. *J Biomed Opt.* (2021) 26:020502. doi: 10.1117/1.JBO.26.2.020502
18. Singh M, Wu C, Liu CH, Li J, Schill A, Nair A, et al. Phase-sensitive optical coherence elastography at 1.5 million A-Lines per second. *Opt Lett.* (2015) 40:2588–91. doi: 10.1364/OL.40.002588
19. Singh M, Schill AW, Nair A, Aglyamov SR, Larina IV, Larin KV. Ultra-fast dynamic line-field optical coherence elastography. *Opt Lett.* (2021) 46:4742–4. doi: 10.1364/OL.435278
20. Nair A, Singh M, Aglyamov SR, Larin KV. Heartbeat OCE: corneal biomechanical response to simulated heartbeat pulsation measured by optical coherence elastography. *J Biomed Opt.* (2020) 25:1–9. doi: 10.1117/1.JBO.25.5.055001
21. Zaitsev VY, Matveyev AL, Matveev LA, Sovetsky AA, Hepburn MS, Mowla A, et al. Strain and elasticity imaging in compression optical coherence elastography: the two-decade perspective and recent advances. *J Biophotonics.* (2021) 14:e202000257. doi: 10.1002/jbio.202000257
22. Ambekar YS, Singh M, Zhang J, Nair A, Aglyamov SR, Scarcelli G, et al. Multimodal quantitative optical elastography of the crystalline lens with optical coherence elastography and Brillouin microscopy. *Biomed Opt Express.* (2020) 11:2041–51. doi: 10.1364/BOE.387361
23. Willekens K, Rocha R, Van Keer K, Vandewalle E, Abegao Pinto L, Stalmans I, et al. Review on dynamic contour tonometry and ocular pulse amplitude. *Ophthalmic Res.* (2015) 55:91–8. doi: 10.1159/000441796
24. Sticker M, Hitzberger CK, Leitgeb R, Fercher AF. Quantitative differential phase measurement and imaging in transparent and turbid media by optical coherence tomography. *Opt Lett.* (2001) 26:518–20. doi: 10.1364/ol.26.000518
25. Lan G, Singh M, Larin KV, Twa MD. Common-path phase-sensitive optical coherence tomography provides enhanced phase stability and detection sensitivity for dynamic elastography. *Biomed Opt Express.* (2017) 8:5253–66. doi: 10.1364/BOE.8.005253
26. Kennedy BF, McLaughlin RA, Kennedy KM, Chin L, Curatolo A, Tien A, et al. Optical coherence micro-elastography: mechanical-contrast imaging of tissue microstructure. *Biomed Opt Express.* (2014) 5:2113–24. doi: 10.1364/BOE.5.002113
27. Zvietcovich F, Rolland J, Yao J, Meemon P, Parker K. Comparative study of shear wave-based elastography techniques in optical coherence tomography. *J Biomed Opt.* (2017) 22:035010. doi: 10.1117/1.JBO.22.3.035010
28. Matveyev AL, Matveev LA, Sovetsky AA, Gelikonov GV, Moiseev AA, Zaitsev VY. Vector method for strain estimation in phase-sensitive optical coherence elastography. *Laser Phys Lett.* (2018) 15:065603. doi: 10.1364/OL.446403
29. Mandell RB. Corneal power correction factor for photorefractive keratectomy. *J Refract Corneal Surg.* (1994) 10:125–8. doi: 10.3928/1081-597x-19940301-11
30. Kennedy BF, Koh SH, McLaughlin RA, Kennedy KM, Munro PR, Sampson DD. Strain estimation in phase-sensitive optical coherence elastography. *Biomed Opt Express.* (2012) 3:1865–79. doi: 10.1364/boe.3.001865
31. Wollensak G, Spoerl E, Seiler T. Riboflavin/ultraviolet-a-induced collagen crosslinking for the treatment of keratoconus. *Am J Ophthalmol.* (2003) 135:620–7. doi: 10.1016/s0002-9394(02)02220-1

32. Singh M, Li J, Vantipalli S, Wang S, Han Z, Nair A, et al. Noncontact elastic wave imaging optical coherence elastography for evaluating changes in corneal elasticity due to crosslinking. *IEEE J Sel Top Quantum Electron.* (2016) 22:266–76. doi: 10.1109/JSTQE.2015.2510293
33. Hepburn MS, Wijesinghe P, Chin L, Kennedy BF. Analysis of spatial resolution in phase-sensitive compression optical coherence elastography. *Biomed Opt Express.* (2019) 10:1496–513. doi: 10.1364/BOE.10.001496
34. Hepburn MS, Foo KY, Wijesinghe P, Munro PRT, Chin L, Kennedy BF. Speckle-dependent accuracy in phase-sensitive optical coherence tomography. *Opt Express.* (2021) 29:16950–68. doi: 10.1364/OE.417954
35. Baptista AMG, De Sousa RARC, Serra PM, Abreu CMDs, Da Silva CMLR. Evaluation of discomfort of Goldmann tonometry without anaesthetic. *Ophthalmic Physiol Opt.* (2010) 30:854–9. doi: 10.1111/j.1475-1313.2010.00786.x
36. De Stefano VS, Ford MR, Seven I, Dupps WJ Jr. Live human assessment of depth-dependent corneal displacements with swept-source optical coherence elastography. *PLoS One.* (2018) 13:e0209480. doi: 10.1371/journal.pone.0209480
37. Li E, Makita S, Azuma S, Miyazawa A, Yasuno Y. Compression optical coherence elastography with two-dimensional displacement measurement and local deformation visualization. *Opt Lett.* (2019) 44:787–90. doi: 10.1364/OL.44.000787
38. Kurokawa K, Makita S, Hong Y-J, Yasuno Y. In-plane and out-of-plane tissue micro-displacement measurement by correlation coefficients of optical coherence tomography. *Opt Lett.* (2015) 40:2153–6. doi: 10.1364/OL.40.002153
39. Kennedy KM, Chin L, McLaughlin RA, Latham B, Saunders CM, Sampson DD, et al. Quantitative micro-elastography: imaging of tissue elasticity using compression optical coherence elastography. *Sci Rep.* (2015) 5:15538. doi: 10.1038/srep15538

Conflict of Interest: The authors declare that the research was conducted in the absence of any commercial or financial relationships that could be construed as a potential conflict of interest.

Publisher's Note: All claims expressed in this article are solely those of the authors and do not necessarily represent those of their affiliated organizations, or those of the publisher, the editors and the reviewers. Any product that may be evaluated in this article, or claim that may be made by its manufacturer, is not guaranteed or endorsed by the publisher.

Copyright © 2022 Nair, Singh, Aglyamov and Larin. This is an open-access article distributed under the terms of the Creative Commons Attribution License (CC BY). The use, distribution or reproduction in other forums is permitted, provided the original author(s) and the copyright owner(s) are credited and that the original publication in this journal is cited, in accordance with accepted academic practice. No use, distribution or reproduction is permitted which does not comply with these terms.